Check for updates

**Proceedings of the ASME 2020**
**International Design Engineering Technical Conferences**
**and Computers and Information in Engineering Conference**
**IDETC/CIE2020**
**August 17-19, 2020, Virtual, Online**

**DETC2020-22725**

Downloaded from http://asmedigitalcollection.asme.org/IDETC-CIE/proceedings-pdf/IDETC-CIE2020/84003/V11AT11A034/6587146/v11at11a034-detc2020-22725.pdf by University Of Wisconsin Madison user on 08 February 2021

# ENHANCED TOOLPATH PLANNING FOR FUSED FILAMENT FABRICATION

**Hongrui Chen**
Department of Mechanical Engineering
University of Wisconsin-Madison
Madison, Wisconsin 53706
Email: hchen496@wisc.edu

**Xingchen Liu***
International Computer Science Institute
Berkeley, California, 94704
Email: xingchen@icsi.berkeley.edu

## ABSTRACT

The slicing software process the 3D geometry into 2D slices and toolpaths for additive manufacturing processes. Most slicing software allows users to select from an array of infill patterns and to specify the overall infill volume fraction globally. However, the ability to locally control the volume fraction, and mechanical properties, is often limited. In this paper, we propose a novel toolpath enhancing algorithm to enable the local control on the volume fraction of various stock and custom infill patterns. In particular, the algorithm widens the infill pattern by directly modifying their toolpath with connected Fermat curves. By preserving the topology of the original toolpath, the connected Fermat curve not only produces predictable boosts in part performance but also minimized the printing time by eliminating extruder traversals without material deposition. The field that controls local volume fraction can be designed either manually or through optimization. The effectiveness of the proposed approach in toolpath generation is demonstrated through volume fraction fields designed by both approaches.

## 1 INTRODUCTION

Additive Manufacturing (AM) creates the model by placing materials layer by layer. This characteristic of AM enables the creation of internally hollow structures. The hollow internal structure reduces the weight of the part, meanwhile maintaining comparable mechanical performances comparable to solid structures. Fused Filament Fabrication (FFF) is a widely available technology of AM. FFF uses toolpath instruction to guide an extrusion head depositing polymer along the path. To create such toolpaths, slicing algorithms were developed. The slicing algorithm converts the 3D model, usually in the form of a triangular mesh, to 2D contours. To reduce the amount of material required and reduce printing time, the solid inside of the 3D model are often replaced by infill structures, which are generated slice by slice inside the 2D contours.

Hidden inside the printed model, infill structures provide engineers additional design freedom without affecting the overall geometry of the model. As shown in Figure 2, an array of infill structures are often readily available in popular slicing software. These different infill structures can directly affect the mechanical property of the part and are important design variables to choose for the slicing algorithm. What's more, the ability to create local variation in infill structures enables the local variation in weight and mechanical property with in the part. This capability is invaluable as it, in its most simple form, allows designers to add material to place needed and subtract not needed. However, to the best of our knowledge, most popular slicing algorithms only allow the specification of a global volume fraction of the infill structure [1,2], while very few can rely on a field to generate locally varying density infill patterns [3,4].

In this paper, we developed a novel method of creating local variation among infill structures by directly modifying the printing path tailoring to a given relative density (volume fraction) field. With the relationship between stiffness tensor and relative density, such a field may be generated by a structural optimization [5]. Alternatively, local volume fraction may be associated with the

*Address all correspondence to this author.



Copyright © 2020 ASME

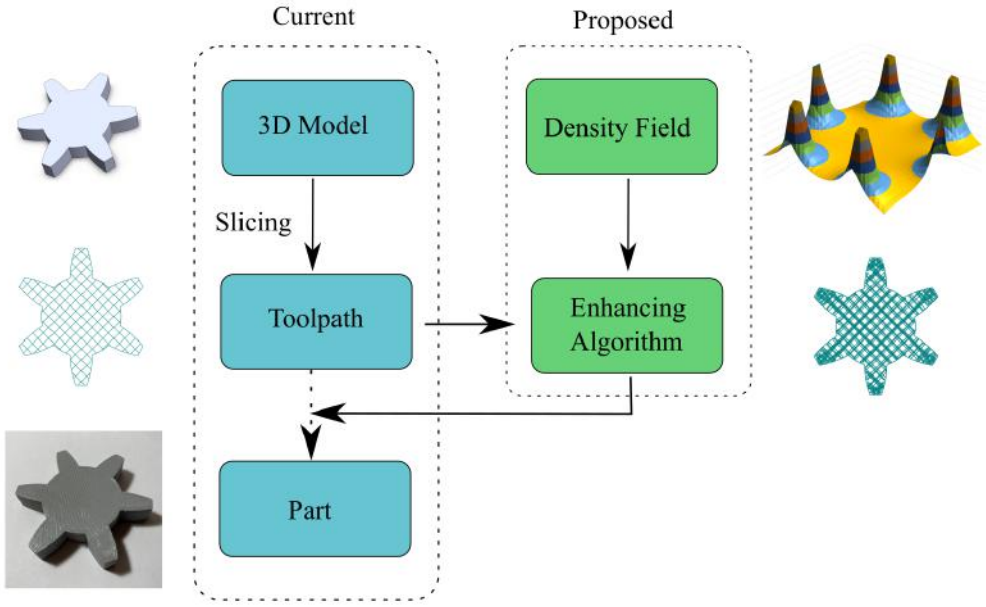



**FIGURE 1**: Flowchart of the toolpath enhancing algorithm (green) and its integration with the current FFF manufacturing pipeline (blue). The dashed arrow in the existing pipeline is replaced by the proposed toolpath enhancing algorithm. The input density field can be generated through structural optimization. It can also be designed manually.

maximum principal stress resulting from a finite element simulation, i.e. higher volume fraction for areas with high stresses. In addition, we implement a manual design tool based on inverse distance interpolation [6]. We then locally modify the width of the infill structure by offsetting the toolpath with contours based on the density value from the field. The contours are then offset with a constant distance repeatedly until the entire space is filled. We call the offsetting contours "contour-parallel" toolpaths. The contour parallel paths are cut and connected to form Fermat curves (see Figure 5 for details).

The proposed approach neatly integrates with the existing FFF manufacturing workflow. As shown in Figure 1, current FFF manufacturing begins with the 3D model. The model is then processed by a slicer to create toolpaths in layers, which are input to the proposed approach. Finally, a FFF printer will follow the toolpath and create the physical model.

The resulting toolpath preserves the original geometry but with an improved infill structure (Figure 3). The property of Fermat curves preserves the original topology of the infill toolpath, which has two benefits. First, a continuous path minimizes the tool head traversing between the endpoint of the current toolpath to the start point of the next toolpath segment without depositing materials that contribute to the actual model (Figure 4). Second, self-intersection within the same layer can cause the material to be deposited on a single point multiple times, resulting in the material to stack up and affect printing quality. Such property ensures that the generated toolpath does not introduce additional self-intersections.

The rest of the paper is organized as follows: In Section 2, we review the previous research related to creating infill structures based on relative density fields and the procedure of creating Fermat curves. In Section 3, we introduce the toolpath enhancing algorithm that modifies the uniform toolpath with the given relative density field. We present three test cases in Section 4 to demonstrate the capability of the algorithm. Section 5 concludes with a discussion.

## 2 BACKGROUND AND RELATED WORK

In FFF, slicing algorithms, also known as "slicer", convert 3D models to toolpaths for the 3D printer. In the present work, we used Cura [1] as an example for the discussion. However, the arguments apply to other open-source slicers, such as Slic3r [2], as well. Cura provides several infill patterns which are shown in Figure 2. During slicing, users specify the density of the infill pattern which, in turn, determines the distance between printing paths given the width of the extrusion [7]. These infill patterns help create extra design freedoms without sacrificing the mechanical performance of the part. Albeit straightforward, the density of these infill patterns can only be specified globally in the state-of-the-art slicers.

Recently, several methods have been proposed to create infill patterns that are capable of local variations. These methods can be broadly put into two categories, depending on whether fur-

Downloaded from http://asmedigitalcollection.asme.org/IDETC-CIE/proceedings-pdf/IDETC-CIE2020/84003/V11AT11A034/6587146/v11at11a034-detc2020-22725.pdf by University Of Wisconsin Madison user on 08 February 2021


Copyright © 2020 ASME

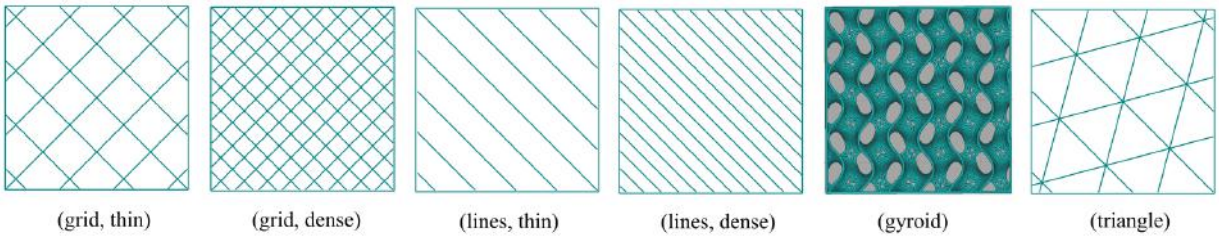



**FIGURE 2**: Commonly available infill patterns among the state-of-the-art slices."Thin" refers to a low global density value and "dense" refers to a high global density value.

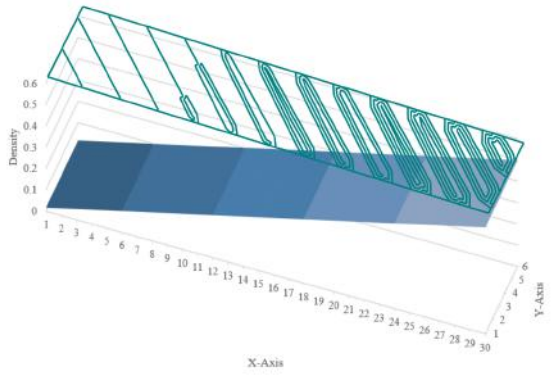



**FIGURE 3**: Demonstration of the toolpath enhancing algorithm on a linearly increasing density field. The sliced toolpath lies in the X-Y plane and Z axis indicates the density value. The shade of blue corresponds to a range in density values.

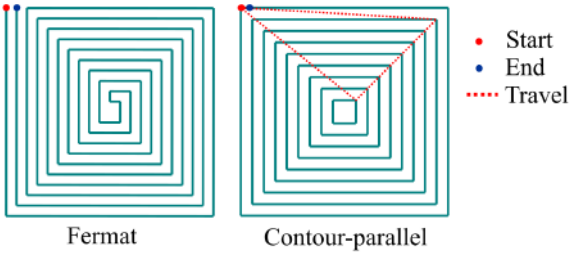



**FIGURE 4**: Comparing to contour-parallel toolpath, Fermat curve toolpath eliminates the repeated starts and stops of the printhead.

ther path planning is required before manufacturing. In the first category, algorithms design toolpath directly and no additional planning is required. For example, Steuben et. al. developed an implicit slicer that uses the level set of stress fields to create toolpath [3]. Followed by the recent development of the implicit slicer by integrating topology optimization tools [8]. Kuipers et. al. generated toolpath for foam like infill structure with graded density [9]. Toolpath level optimization has also been used to create more accurate geometry by adaptive width control of extrusion [10]. Our algorithm enhances toolpath directly and can be used in conjunction with any of these methods referenced above.

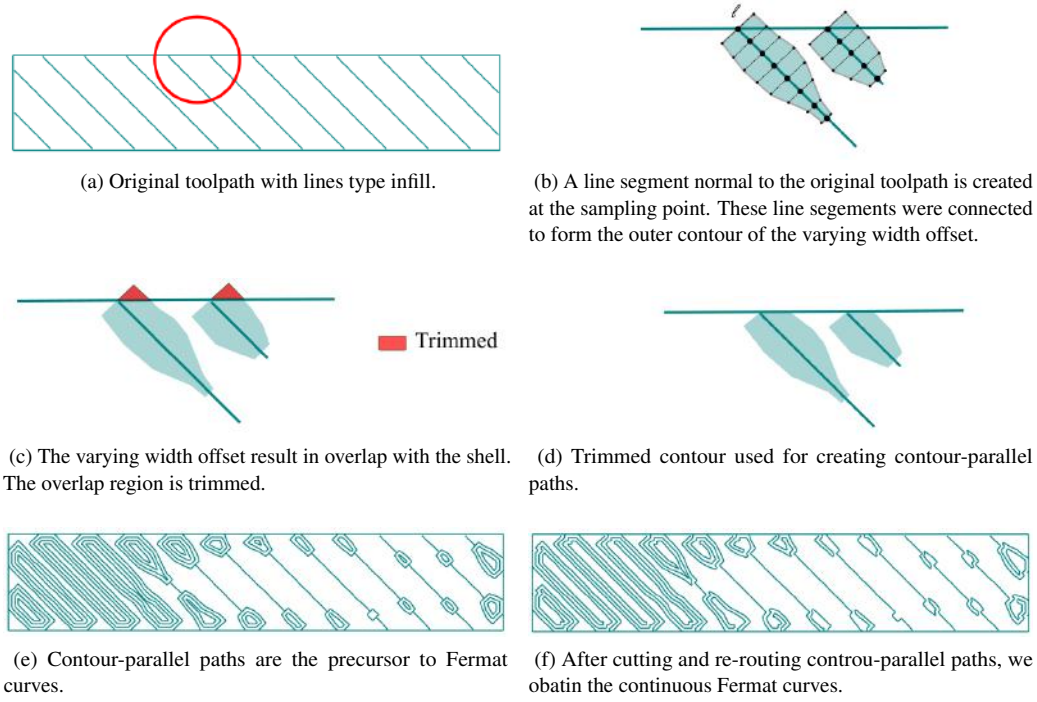
A majority of infill design methods are in the second category that focuses on the (pre-path planned) geometry of the infill structure. As a result, these infill structures may not be accurately reproduced and errors may be introduced during the path planning stage given the small size of the infill structure and the finite resolution of the FFF printing nozzle diameter. Without being exhaustive, the following is a list of the related work. Schumacher et. al. and Panetta et. al created internal unit cell structures to generate models with spatially variable stiffness property [11, 12]. Martínez et. al. developed a method of using Voronoi foam to procedural generate microstructure depending on a relative density field [13]. Stava et. al. developed a system that automatic hollows, thickens, and inserts struts to the model [14]. Zhou and Li proposed an inverse homogenization methodology for microstructure design for functionally graded material [15]. Li et. al. generated porous structures based on implicit functions for the interior structure [16]. Pasko et. al. proposed a new approach of generating heterogeneous objects with internal volumetric structures [17]. Wu et. al. generated a bone-like infill structure based on voxel-wise topology optimization [18]. Our toolpath enhancing algorithm is fundamentally different from these approaches in that we modify the toolpath directly and these changes will be correctly reflected on the final printed part.

## 3 TOOLPATH ENHANCING ALGORITHM

Our goal is to develop a general method to enhance the toolpath of various commonly used infill structures. The algorithm modifies the width of the infill structures according to the given density fields while maintaining the topology of the original toolpath. To achieve this goal, we first load in the toolpath generated by slices or any other toolpath planning algorithm. The original single-track toolpaths are then dilated into contour-parallels according to the given (relative) density field. Last, we connect each set of contour-parallels into single connected Fermat curves. The toolpaths enhancing algorithm only modifies the infill structure thus leaves the overall geometry of the part intact.

Downloaded from http://asmedigitalcollection.asme.org/IDETC-CIE/proceedings-pdf/IDETC-CIE2020/84003/V11AT11A034/6587146/v11at11a034-detc2020-22725.pdf by University Of Wisconsin Madison user on 08 February 2021


Copyright © 2020 ASME




(a) Original toolpath with lines type infill.

(b) A line segment normal to the original toolpath is created at the sampling point. These line segements were connected to form the outer contour of the varying width offset.

(c) The varying width offset result in overlap with the shell. The overlap region is trimmed.

(d) Trimmed contour used for creating contour-parallel paths.

(e) Contour-parallel paths are the precursor to Fermat curves.

(f) After cutting and re-routing controu-parallel paths, we obatin the continuous Fermat curves.

**FIGURE 5**: Overview of toolpath enhancing algorithm. The algorithm begins with importing the original toolpath and modify only the infill toolpath by varying their width. The the modified toolpath will be trimmed to maintain the same geometry. We use Fermat curves to fill the varying width sections.

### 3.1 Load the Original Toolpath

The proposed method aims to enhance the existing infill toolpath for better mechanical performance. As shown in Figure 6, most FFF printed structures contain a solid outer shell and an internal sparse infill. The proposed algorithm only modifies the infill toolpaths to control the local density of the infill structure. Some slicers annotated the toolpaths for shell and infill. For example, Cura labels infill toolpath with ";TYPE:INFILL" and shell toolpath with ";TYPE:WALL-OUTER" and ";TYPE:WALL-INTER". If such annotation is unavailable, additional steps to separate the two types of toolpath may be required. For example, the infill toolpath can be identified through an offset of the original shape of the part. Alternatively, we can clamp the density field such that the density value over the shell toolpath becomes undefined, leaving the shell toolpath undisturbed. In the rest of the paper, we assume the toolpath is annotated and the toolpath for infill and shell are already separated.

### 3.2 Create Varying Distance Offset

We create the varying distance offset by dilating the original single-track toolpaths into contour-parallels according to the given (relative) density field. The density may be generated manually or by structural optimization (see Section 4 for details). The program first iterates through all the infill toolpaths. Along with each infill toolpaths, we sample the density field at a constant distance interval. We sample the density field every 1 mm, balancing between detail in geometry and program run time. For the density field defined at a lower resolution, we smooth the density with tri-linear interpolation.

After obtaining the density at the sampling point, we create a varying distance offset algorithm to alter the width of the toolpath by offsetting points. A line segment normal to the original toolpath is created at the sampling point. The length of the line segment is calculated with the following equation:

$$l(x,y,z) = \rho(x,y,z) d_{infill} \tag{1}$$

Where $l(x,y,z)$ is the length of the line segment. $\rho$ is the density at point $(x,y,z)$. $d_{infill}$ is the separation distance between each line of the infill toolpath. For example, two parallel lines with a distance of 4mm results in a $d_{infill}$ of 4. In Cura (and other common slicers), this distance is a value calculated based on the infill density setting or in reverse, used as a parameter to determine the infill density. The center of the normal line coincides with the original infill toolpath. We obtain two offset points from


Copyright © 2020 ASME

Downloaded from http://asmedigitalcollection.asme.org/IDETC-CIE/proceedings-pdf/IDETC-CIE2020/84003/V11AT11A034/6587146/v11at11a034-detc2020-22725.pdf by University Of Wisconsin Madison user on 08 February 2021

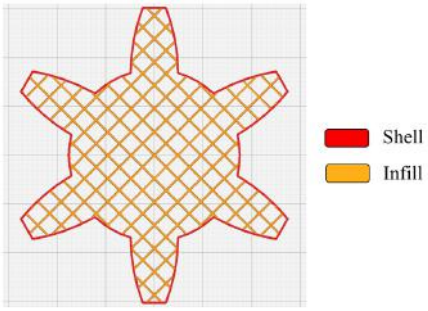
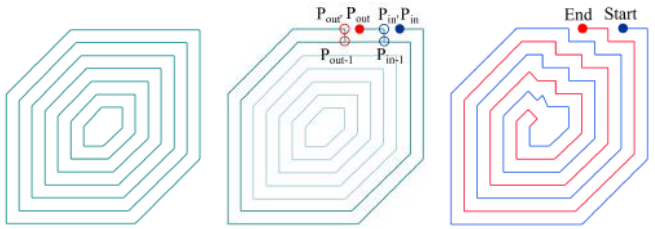



**FIGURE 6**: The FFF toolpath consists of two regions: shell and infill. The shell defines the geometry and infill fills the area encapsulated by the shell.




(a) Contour-parallel paths. (b) Cutting and rerouting contours. (c) Finished Fermat Curve.

**FIGURE 7**: Steps of connecting contour-parallels into Fermat curves. (a) From the outer most contour, we repeatedly create equal distance $d$ offset of the outer contour. The resulting paths is a contour-parallel toolpath. (b) From start point $P_{in}$ and end point $P_{out}$, $P_{in'}$ and $P_{out'}$ is at distance $d$ from $P_{in}$ and $P_{out}$ along the same contour. Two perpendicular paths are then created from $P_{in'}$ and $P_{out'}$ to the next level of contour inside. The intersection is $P_{in-1}$ and $P_{out-1}$ . $P_{in-1}$ and $P_{out-1}$ become the new $P_{in}$ and $P_{out}$; the process will repeat itself until it reaches the innermost contour. (c) The resulting geometry is continuous Fermat curve.

the endpoint of the normal line. This process is repeated for all sampling points on every infill toolpath.

This process results in one quadrilateral per each neighboring pair of line segments. When creating varying width offset for infill toolpath with sharp corners, it is possible that two normal lines overlaps with each other and create an ”x” shape. In this case, the order of points are rearranged so that a quadrilateral can still be formed. We specified a threshold such that no offset is created for density values less than 0.1. The threshold prevents the generation of overlapping offset lines. Last, we union all quadrilaterals with the Clipper library [19].

Sometimes, results from variable width offset overlap with the shell. From our experience, these overlaps often occur towards the end or start of a toolpath where the sampling points are closest to the shell. The shell can locate on either the outside or inside of a part when holes exist. Shown in Figure 5(c), for shell toolpath located on the outside, a Boolean intersection trims down the overlapping region. For shell toolpath located on the inside of the model, a Boolean difference trims down regions located inside the shell.

Since the original toolpaths do not contain information about whether the shell toolpaths are located on the outside or the inside, we designed a heuristic method to determine the result of these Boolean operations. We first perform both Boolean intersection and difference with Clipper between each varying width segment. We then keep the result with a higher number of vertices from the two Boolean operations since we observed that the discarded section always contains fewer vertices compared to the section to be retained. Therefore, This output trimmed contour is shown in Figure 5(d).

### 3.3 Adapting Field with Fermat Curve

For FFF toolpath, long, continuous toolpaths are often preferred over short, discontinuous ones that result in constant starts and stops of the printhead. When printing disconnected segments, the printhead needs to stop extrusion of materials, then retract the filament for some distance to prevent the material from oozing out of the nozzle during traversals before moving to the start of the next segment and extruding again. This process could slow down the print process by adding movements that are not contributing to the printed model. Continuous toolpath saves the tool head from retraction and traversal between sections of disconnected toolpaths segments. For this reason, space-filling curves, such as Hilbert curves, are often used to generate infill toolpath. Recently, connected Fermat curves were introduced to generate the printing toolpath for FFF slices [20].

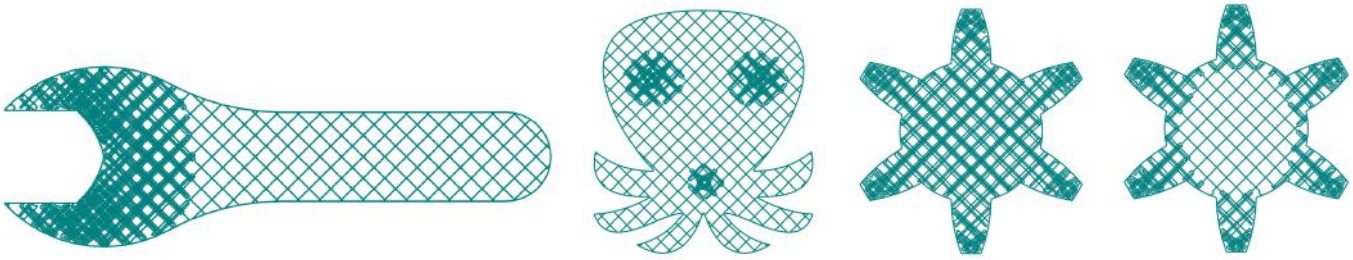
Several algorithms have been proposed to generate connected Fermat curves [20,21]. These researches focus on creating Fermat curves that completely fill a given space. While demonstrating great results in creating continuous toolpaths, they differ from the common infill toolpath geometries which could pose difficulties when incorporating the current pipeline of FFF.

The Fermat curve generation algorithm in this paper is a combination of the method referenced above. As shown in Figure 7(a), from the outermost contour, we repeatedly create equal distance $d$ offset of the outer contour. The resulting path is a contour-parallel toolpath. On the outermost, we specify a start point $P_{in}$ and an endpoint $P_{out}$. Along the same contour, we locate $P_{in'}$ and $P_{out'}$ at distance $d$ from $P_{in}$ and $P_{out}$. The path between $P_{in}P_{in'}$ and $P_{out}P_{out'}$ is cut. Two perpendicular paths are then created from $P_{in'}$ and $P_{out'}$ to the next level of contour inside where we obtain two intersecting points. We name the two points as $P_{in-1}$ and $P_{out-1}$. $P_{in-1}$ and $P_{out-1}$ becomes the new $P_{in}$ and $P_{out}$; the process repeats itself until it reaches the innermost contour. The resulting geometry is a continuous Fermat curve.

Downloaded from http://asmedigitalcollection.asme.org/IDETC-CIE/proceedings-pdf/IDETC-CIE2020/84003/V11AT11A034/6587146/v11at11a034-detc2020-22725.pdf by University Of Wisconsin Madison user on 08 February 2021

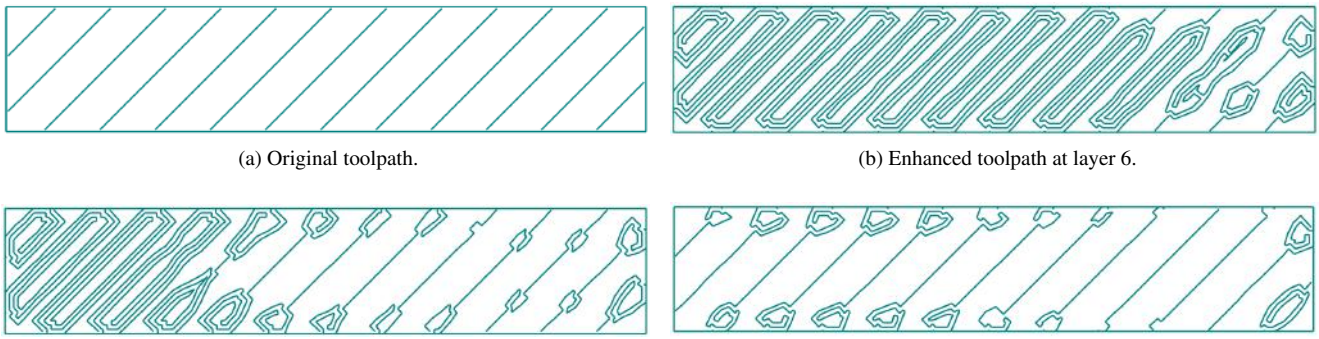


Copyright © 2020 ASME



(a) Wrench. (b) Octopus. (c) Gear with high density infill. (d) Gear with low density infill in the center.

**FIGURE 8**: The user can manually select points inside the toolpath domain to assign weight values.



(a) Original toolpath. (b) Enhanced toolpath at layer 6.

(c) Enhanced toolpath at layer 13. (d) Enhanced toolpath at layer 24.

**FIGURE 9**: Comparison between the original toolpath and the enhanced toolpath with lines type infill. Layer 6, 13, and 24 are shown out of 99 layers.

Zhao et. al.'s method requires the creation of a spiral path from contour-parallel paths as a precursor to Fermat curves. Therefore, we used the method from Zhai et. al.'s paper to locate the inner points. Zhai et. al.'s process requires an additional toolpath to be added to maintain continuity. In the case of FFF, an additional toolpath inside the equal distance contours could cause extra material to be deposited. Zhao et. al. remove a segment from the innermost contour which could be more beneficial for the FFF process. Therefore, we use Zhao et. al.'s method for processing the innermost contour.

We preserve the topology of the original toolpaths by keeping the start and endpoints of each continuous toolpath (see Figure 5(f)). The proposed algorithm creates continuous Fermat curves for every varying width segment and iterates through all the layers created by the slicer.

## 4 DEMONSTRATION RESULTS

The toolpath enhancing algorithm is implemented in C++. We use Cura 4.5 from Ultimaker B.V. to generate the original toolpath [1]. We printed the model on a custom-designed printer with a nozzle diameter of 0.4 [mm]. The material is grey Polylactic Acid (PLA) filament. Two test cases were created to demonstrate the capabilities of the toolpath enhancing algorithm. In the first test case, we demonstrated that the user can manually select points inside the toolpath domain to assign weight values. In the second test case, we set up a simple optimization example to generate a density field. In addition, we use Top3D to optimize the model from the second test case by removing sections with low-density value.

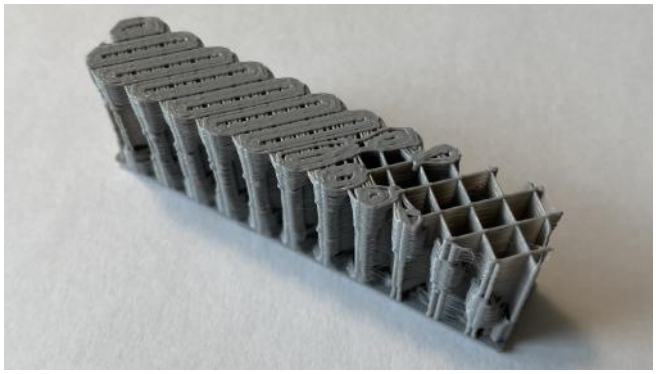
### 4.1 Manually Designed Density Field

Currently, the inputs of slicers are stereolithography (STL) models. Stereolithography models only contain information about the geometry of the model. Most slicers take the geometry model and perform slicing algorithms purely based on geometry. Slicers do not offer the ability to conduct FEA or other simulations that can generate a density field. One way to integrate the toolpath enhancing algorithm is to create it as an add on to common slicers.

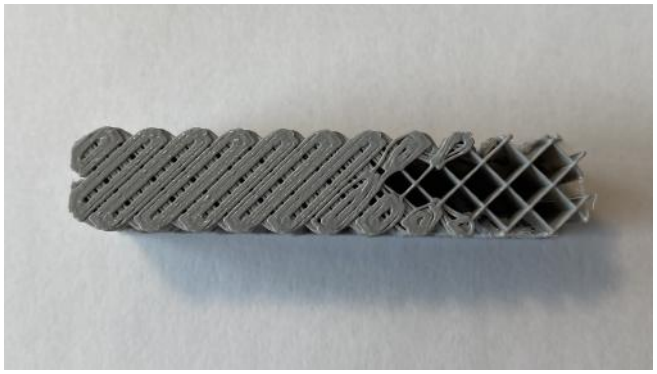
Inside the toolpath enhancing program, the user can specify points to define regions where they want the density to be altered.


Copyright © 2020 ASME

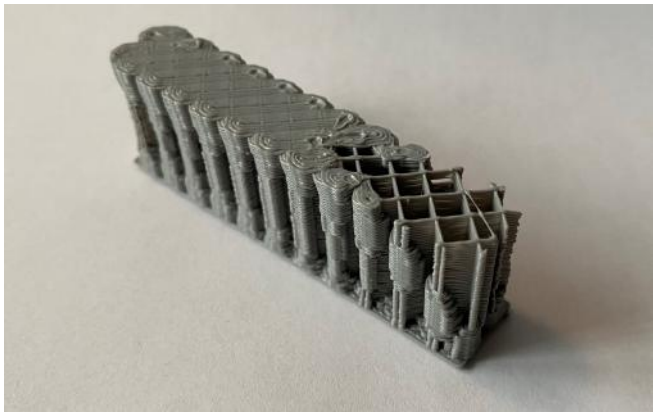
Downloaded from http://asmedigitalcollection.asme.org/IDETC-CIE/proceedings-pdf/IDETC-CIE2020/84003/V11AT11A034/6587146/v11at11a034-detc2020-22725.pdf by University Of Wisconsin Madison user on 08 February 2021



(a) Fermat curves toolpath side view.



(b) Fermat curves toolpath top view.



(c) Contour-parallel toolpath side view.



(d) Contour-parallel toolpath top view.

**FIGURE 10**: Printed result from the toolpath enhancing algorithm. For better visulization of the infill structure, we removed the shell toolpaths. (a) and (b) are generated with Fermat curves. (c) and (d) is generated with contour-parallel curves. Viewed from the top, the print quality of Fermat curves is better.

This allows users to use more sparse infill and increase the infill density in regions with thin features or high stress. On the other hand, the user can also begin with more dense infill and specify regions where lower density is desired. The program cutoff any value above 1 and below 0 by default.

We implement the following equations to perform inverse distance interpolation for the manual design of the density field:

$$w(x) = \begin{cases} \sum_{i=1}^{n} w_i(x) u_i & \text{if } d(x,x_i) \neq 0 \text{ for all } i, \\ u_i & \text{if } d(x,x_i) = 0 \text{ for some } i, \end{cases} \tag{2}$$

where

$$w_i(x) = \frac{1}{d(x,x_i)^2} \tag{3}$$

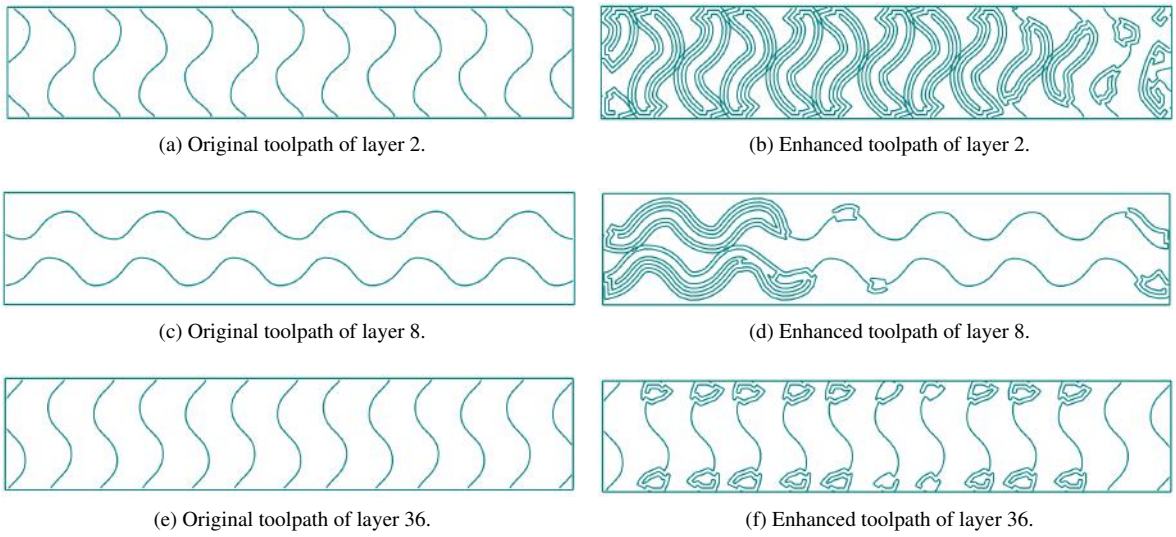
This equation is based on Shepard's method [6]. With the original Shepard's method, if there is only one value defined in space, the entire space is interpolated to that value. We modified it such that there is a decay of density value as distance increases. In the equation, $u_i$ is the user-specified density value at a point $x_i$. $x$ is the point where the density value is currently being calculated. $d(x,x_i)$ is the distance between point $x_i$ to the point $x$ and $N$ is the total number of user-specified points. $w(x)$ is the final relative density value at point $x$.

Shown in Figure 8, we created several toolpaths with manually designed density fields. The models were created with SolidWorks and sliced with Cura. In Figure 8(a), we created a wrench with grid-style infill. For the application of a wrench, one can estimate that there could be a high structural load located in the opening section. Two points were added around the openings with a density value of 2.0. Using density larger than 1 artificially increases the weight of that density since all density values kept in the range of 0 to 1. This results in a more dense infill around



Copyright © 2020 ASME

Downloaded from http://asmedigitalcollection.asme.org/IDETC-CIE/proceedings-pdf/IDETC-CIE2020/84003/V11AT11A034/6587146/v11at11a034-detc2020-22725.pdf by University Of Wisconsin Madison user on 08 February 2021



(a) Original toolpath of layer 2.
(b) Enhanced toolpath of layer 2.
(c) Original toolpath of layer 8.
(d) Enhanced toolpath of layer 8.
(e) Original toolpath of layer 36.
(f) Enhanced toolpath of layer 36.

**FIGURE 11**: Comparison between original and enhanced toolpath of a bar with gyroid infill. Total layer count is 49.

the opening. Potentially increasing the rigidity of the part.

In Figure 8(b), we used the toolpath enhancing algorithm to alter the aesthetic of the model. Two points located on the top of the model with a density value of 1.7 were entered to create the eyes of the octopus and one point with a density of 1.0 was entered for the mouth section.

Toolpaths of gears shown in Figure 8(c) and (d) are enhanced the density field such that six points with density values of 1.7 are entered in each of the spur regions. The close proximity of the six weights increased the density at the center of the gear. To mitigate this, we use a negative density ( -0.8) to further decrease the density near the center of the gear. With the addition of the negative density, the center section of of 8(d) have loose infill compared to the gear in 8(c).

### 4.2 Optimized Field

In the second test case, we demonstrate that the toolpath enhancing algorithm with a density field that is a result of structural optimization. We assume a nearly linear relationship between the density and stiffness of the infill structure. We note that a better approximation may be obtained, but is outside the scope of the current discussion. Interested reader may refer [22, 5].

In the optimization, we constrained one face and applied a load on a bottom edge. The optimization runs at a resolution of $30\times6\times10$ resolution with a total of 1800 elements. After the optimization, we obtained a density value of each element in the beam. The values are converted into a density field. The density is then inputted into the field adapting algorithm.

We modeled a cube with a dimension of $60\times12\times20$ [mm]. We first sliced a model with straight lines as infill. In Cura, we selected ”lines” for the type of infill and a density of 12%. The infill line distance calculated by Cura is 3.33 [mm]. The sliced toolpaths consist of 99 layers in total. The program takes on average between 30 to 50 seconds to run depending on the complexity of the toolpaths and the density field.

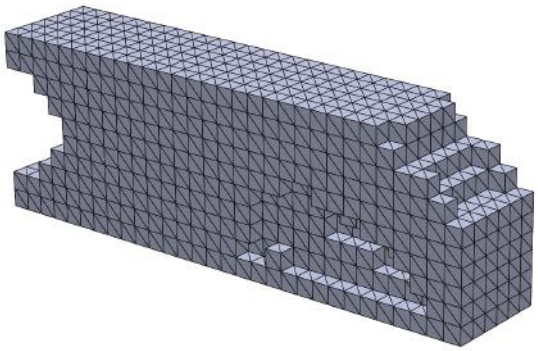
Figure 9(a) shows the original toolpath. The layer is shown in Figure 9(b) is located at the bottom of the model at layer 3 where the overall density is high. Figure 9(d) is layer 12 located in the middle of the model. The density field is greater on the edge. Figure 9 is layer 7 located in between. We observed that the enhanced toolpath resembles the optimization result. For the printing process, we set a nozzle temperature of 210 °C, the print speed to 1000 [mm/min] and we enable retraction of 2 [mm] for travel distance longer than 2 [mm]. This means that retraction will be enabled between each line of infill but not enabled for traversing contours within a varying width segment. The retraction speed is set to 4000 [mm/min]. For the printed models, we used a layer height of 0.2 [mm] resulting in 99 total layers.

To further demonstrate the performance of the proposed approach, we also generated an enhanced toolpath with contour-parallel curves. We printed both the toolpaths and recorded a print time of 1:06:55 for the contour-parallel toolpath and 55:48 for the Fermat curve toolpath, 18% saving in printing time. Also, we observed a better print quality from the Fermat curves toolpath in that the contour-parallel toolpath has artifacts at the innermost contour where the tool head needs to pause and retract to continue printing.

In addition to the line infill, we also configured Cura with gyroid infill. We used an infill density of 10% with an infill line distance of 4.0 [mm]. The implementation of gyroid in Cura


Copyright © 2020 ASME

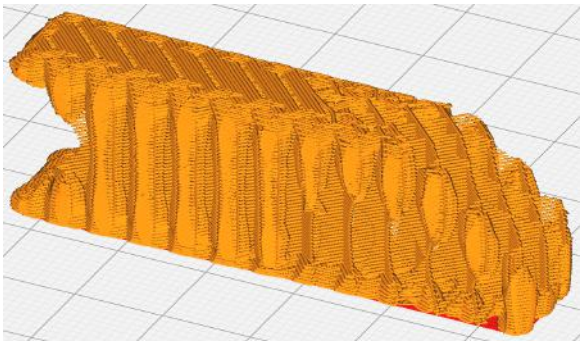
Downloaded from http://asmedigitalcollection.asme.org/IDETC-CIE/proceedings-pdf/IDETC-CIE2020/84003/V11AT11A034/6587146/v11at11a034-detc2020-22725.pdf by University Of Wisconsin Madison user on 08 February 2021



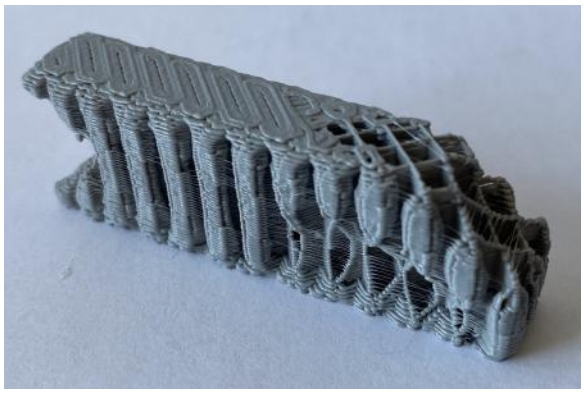
(a) Extracted boundary of the optimized beam by discarding regions with less than 0.2 density.



(b) Further smoothed the mesh to remove overhangs.



(c) Visualization of the enhanced toolpath.



(d) Printed structure with removed shell section for better visibility of the infill structure.

**FIGURE 12**: There are regions with very low to zero density value from the optimization result. We optimized the model by trimming the regions with low-density value which decreased the material use.

consists of many short straight line segments to form the overall curvy structure. The gyroid infill also consists of tight radius turns. Shown in Figure 11(b)(d)(f), we presented three selected layers of enhanced gyroid infill and their corresponding original toolpath in Figure 11(a)(c)(e).

From the optimization result, we found out there are regions with very low to zero density value. By trimming the regions with low-density value, the material use of the model can be reduced. Removing regions will also result in a more challenging outer geometry compared to the cube.

We extract the boundary of the optimized beam by discarding regions with less than 0.2 density. We use Top3DSTL to create the STL file for slicing [23]. The output mesh is shown in Figure 12(a). We further smooth the mesh to remove the overhangs. The resulting mesh, shown in Figure 12(b) consists of a more gentle curvature and can be printed without support material. We then slice smoothed mesh in Cura with line fill and infill density of 12%. The resulting enhanced toolpath is shown in Figure 12(c). We removed the shell section for better visibility of the infill structure. The printed result is shown in Figure 12(d).

## 5 CONCLUSION

In this paper, we developed and demonstrated a toolpath enhancing algorithm. This novel method modifies the original infill toolpath by adapting it to a given density field. We demonstrated the toolpath enhancing algorithm over multiple infill patterns. Also, the toolpath enhancing algorithm preserves the original topology through the use of Fermat curves, reducing the amount of retraction and travel needed when traversing disconnected sections of the toolpath.

The current work demonstrates many advantages of the toolpath enhancing algorithm. When incorporated future work discussed above, this method could greatly improve the mechanical property of additive manufactured components. Moreover, it is not limited to the dentistry field as input, but other types of the


Copyright © 2020 ASME

Downloaded from http://asmedigitalcollection.asme.org/IDETC-CIE/proceedings-pdf/IDETC-CIE2020/84003/V11AT11A034/6587146/v11at11a034-detc2020-22725.pdf by University Of Wisconsin Madison user on 08 February 2021

field could also be utilized.

The generated Fermat curves may be further improved for FFF manufacturing with a few post-processing steps. To maintain the original topology of the toolpath, the Fermat curve will leave the innermost contour of each segment with one less line as shown in Figure 5 (e) and (f). By modifying how much materials will be extruded per unit of distance, or extrusion ratio, of the innermost contour, the nozzle can deposit extra materials to fill in the gap.

A heuristic-based density field generation methods may also be developed. As most common slicers cannot conduct structural analysis, using a heuristic to generate the density field could allow the most straightforward experience for users of slicing software.

Last but not the least, the current algorithm creates gaps inside contours to maintain continuity of the curves. We would like to improve the Fermat curve generation algorithm so that the gaps can be avoided.

## Acknowledgements

This research was partially supported by the Defense Advanced Research Projects Agency. The responsibility for errors and omissions lies solely with the author.

## REFERENCES

[1] Ultimaker Cura: Powerful, easy-to-use 3D printing software, n.d., from https://ultimaker.com/software/ultimaker-cura.

[2] Slic3r - Open source 3D printing toolbox, n.d., from https://slic3r.org/.

[3] Steuben, J. C., Iliopoulos, A. P., and Michopoulos, J. G., 2016. "Implicit slicing for functionally tailored additive manufacturing". *CAD Computer Aided Design,* ***77***, aug, pp. 107–119.

[4] Yaman, U., Butt, N., Sacks, E., and Hoffmann, C., 2016. "Slice coherence in a query-based architecture for 3D heterogeneous printing". *CAD Computer Aided Design,* ***75-76***, jun, pp. 27–38.

[5] Liu, X., 2019. "Distributed design of two-scale structures with unit cells". In Proceedings of the ASME Design Engineering Technical Conference, Vol. 2A-2019.

[6] Shepard, D., 1964. "A two-dimensional interpolation for irregularly-spaced data function". *Proc. Ass. Comput. Mach.*, pp. 517–524.

[7] Infill settings – Ultimaker Support, n.d., from https://support.ultimaker.com/hc/en-us/articles/360012607079.

[8] Steuben, J. C., Lliopoulos, A. P., and Michopoulos, J. G., 2017. "Towards multiscale topology optimization for additively manufactured components using implicit slicing". In Proceedings of the ASME Design Engineering Technical Conference, Vol. 1, American Society of Mechanical Engineers (ASME).

[9] Kuipers, T., Wu, J., and Wang, C. C., 2019. "CrossFill: Foam Structures with Graded Density for Continuous Material Extrusion". *CAD Computer Aided Design,* ***114***, sep, pp. 37–50.

[10] Kuipers, T., Doubrovski, E. L., Wu, J., and Wang, C. C., 2020. "A framework for adaptive width control of dense contour-parallel toolpaths in fused deposition modeling". *arXiv preprint arXiv:2004.13497*.

[11] Schumacher, C., Bickel, B., Rys, J., Marschner, S., Daraio, C., and Gross, M., 2015. "Microstructures to Control Elasticity in 3D Printing". *ACM Trans. Graph,* ***34***.

[12] Panetta, J., Zhou, Q., Malomo, L., Pietroni, N., Cignoni, P., and Zorin, D., 2015. "Elastic textures for additive fabrication". In ACM Transactions on Graphics, Vol. 34.

[13] Martínez, J., Dumas, J., and Lefebvre, S., 2016. "Procedural Voronoi Foams for Additive Manufacturing". *ACM Trans. Graph,* ***35***.

[14] Stava, O., Vanek, J., Benes, B., Carr, N., and Měch, R., 2012. "Stress Relief: Improving Structural Strength of 3D Printable Objects". *ACM Trans. Graph,* ***31***(4).

[15] Zhou, S., and Li, Q., 2008. "Design of graded two-phase microstructures for tailored elasticity gradients". *Journal of Materials Science,* ***43***(15), pp. 5157–5167.

[16] Li, D., Dai, N., Jiang, X., and Chen, X., 2016. "Interior structural optimization based on the density-variable shape modeling of 3D printed objects". *International Journal of Advanced Manufacturing Technology,* ***83***(9-12), pp. 1627–1635.

[17] Pasko, A., Fryazinov, O., Vilbrandt, T., Fayolle, P. A., and Adzhiev, V., 2011. "Procedural function-based modelling of volumetric microstructures". *Graphical Models,* ***73***(5), sep, pp. 165–181.

[18] Wu, J., Aage, N., Westermann, R., and Sigmund, O., 2018. "Infill Optimization for Additive Manufacturing-Approaching Bone-Like Porous Structures". *IEEE Transactions on Visualization and Computer Graphics,* ***24***(2), feb, pp. 1127–1140.

[19] Clipper - an open source freeware polygon clipping library.

[20] Zhao, H., Gu, F., Huang, Q. X., Garcia, J., Chen, Y., Tu, C., Benes, B., Zhang, H., Cohen-Or, D., and Chen, B., 2016. "Connected fermat spirals for layered fabrication". In ACM Transactions on Graphics, Vol. 35, Association for Computing Machinery.

[21] Zhai, X., and Chen, F., 2019. "Path Planning of a Type of Porous Structures for Additive Manufacturing". *CAD Computer Aided Design,* ***115***, oct, pp. 218–230.

[22] Liu, X., and Shapiro, V., 2016. "Homogenization of material properties in additively manufactured structures". *CAD Computer Aided Design,* ***78***, sep, pp. 71–82.

[23] Liu, K., and Tovar, A., 2014. "An efficient 3D topology optimization code written in Matlab". *Structural and Multidisciplinary Optimization,* ***50***(6), pp. 1175–1196.

Downloaded from http://asmedigitalcollection.asme.org/IDETC-CIE/proceedings-pdf/IDETC-CIE2020/84003/V11AT11A034/6587146/v11at11a034-detc2020-22725.pdf by University Of Wisconsin Madison user on 08 February 2021



Copyright © 2020 ASME